CISTER
Research Centre in
Real-Time & Embedded
Computing Systems

Conference Paper

Assessing the Interplay between IoT Localization Accuracy and the Two-Ray Channel

Cristobal Huidobro
Miguel Gutiérrez Gaitán*
Christian Oberli
Giovanni Pettorru
Marco Martaló
Virginia Pilloni

*CISTER Research Centre

CISTER-TR-250104

2025/03/24

Assessing the Interplay between IoT Localization Accuracy and the Two-Ray Channel

Cristobal Huidobro, Miguel Gutiérrez Gaitán*, Christian Oberli, Giovanni Pettorru, Marco Martaló, Virginia Pilloni

*CISTER Research Centre

Polytechnic Institute of Porto (ISEP P.Porto)

Rua Dr. António Bernardino de Almeida, 431

4200-072 Porto

Portugal

Tel.: +351.22.8340509, Fax: +351.22.8321159

E-mail: mjggt@isep.ipp.pt, giovanni.pettorru@unica.it, marco.martalo@unica.it, virginia.pilloni@unica.it

https://www.cister-labs.pt

Abstract

This paper analyzes the impact of specular signal reflections on the accuracy of Received Signal Strength (RSS)-based localization for Internet of Things (IoT) devices using the weighted least squares (WLS) regression algorithm within a two-ray propagation channel. Simulations with realistic WiFi/BLE settings, considering distance, antenna heights, and carrier frequency, reveal that localization accuracy is significantly influenced by deep fades caused by surface reflections, which depend on the geometry of anchor-target positions. A pseudo-outlier elimination approach based on feasible localization distances effectively mitigates this issue, significantly reducing localization error. These findings offer practical insights into the performance of WLS-based IoT localization in two-ray environments and lay the groundwork for GPS-free or GPS-denied localization systems in challenging scenarios, such as overwater environments, where two-ray propagation is predominant.

Assessing the Interplay between IoT Localization Accuracy and the Two-Ray Channel

Cristobal Huidobro*, Miguel Gutiérrez Gaitán*†, Christian Oberli*,
Giovanni Pettorru‡, Marco Martaló‡, Virginia Pilloni‡
* Department of Electrical Engineering, Pontificia Universidad Católica de Chile, Chile
Email: {chuidobrr, miguel.gutierrez, obe}@uc.cl
† CISTER Research Centre, Portugal. Email: mjggt@isep.ipp.pt
‡ Department of Electrical and Electronic Engineering, University of Cagliari, Cagliari, Italy.
Email:{giovanni.pettorru,marco.martalo,virginia.pilloni}@unica.it

***Abstract*—This paper analyzes the impact of specular signal reflections on the accuracy of Received Signal Strength (RSS)-based localization for Internet of Things (IoT) devices using the weighted least squares (WLS) regression algorithm within a two-ray propagation channel. Simulations with realistic WiFi/BLE settings, considering distance, antenna heights, and carrier frequency, reveal that localization accuracy is significantly influenced by deep fades caused by surface reflections, which depend on the geometry of anchor-target positions. A pseudo-outlier elimination approach based on feasible localization distances effectively mitigates this issue, significantly reducing localization error. These findings offer practical insights into the performance of WLS-based IoT localization in two-ray environments and lay the groundwork for GPS-free or GPS-denied localization systems in challenging scenarios, such as overwater environments, where two-ray propagation is predominant.**

***Index Terms*—RSSI, Localization, WLS, Two-ray, Regression.**

I. Introduction

The Internet of Things (IoT) paradigm has led to an unprecedented integration of physical devices into interconnected systems across various domains (e.g., smart cities, industrial automation, transportation) and environments (e.g., crop fields, lakes, parking areas), enabling the proliferation of new services and applications. Localization [1] is one critical aspect of modern IoT systems that has paved the way to support IoT applications requiring precise device positioning, such as navigation, asset tracking, and context-aware services.

Traditional methods like GPS, while accurate under certain conditions, are often impractical for many IoT applications due to their high power consumption, cost, and/or availability of satellite visibility (e.g., indoors [2]). Consequently, cost-effective localization methods using commercial off-the-shelf (COTS) devices have garnered significant attention, with Received Signal Strength (RSS)-based [3] localization methods standing out due to their low cost, ease of implementation, and reuse of existing communication infrastructure.

Despite the advantages of RSS-based localization methods, they come with significant limitations and challenges [1], [4]. RSS measurements are highly susceptible to various propagation phenomena, including multipath effects, shadowing, and interference. These phenomena can cause fluctuations in signal strength, leading to inaccuracies in distance estimation and, consequently, localization errors. One of the critical challenges is dealing with ground and surface reflections, which can cause significant signal attenuation. These reflections are particularly problematic in environments with many reflective surfaces, such as parking areas, indoor spaces, and near bodies of water, where the direct line-of-sight (LoS) path is often accompanied by multiple reflected paths.

To address these challenges, advanced yet low-complexity algorithms such as the Weighted Least Squares (WLS) method are often employed [5] [6]. The WLS method extends the classical Least Squares (LS) technique by incorporating weights that reflect the reliability of different measurements. In the context of RSS-based localization, these weights can account for factors like environmental obstacles and distances between the target and reference points, among others. Essentially, by assigning higher weights to more reliable measurements and lower weights to less reliable ones, the WLS algorithm effectively mitigates the adverse effects of typical propagation anomalies, enhancing localization accuracy.

While the WLS-based method has shown to be promising in mitigating some of the challenges associated with RSS-based localization, to the best of our knowledge, the specific impact of a dominant second ray or specular reflections has not been extensively studied. Although other papers may have touched on related topics, they do not address this issue directly. These strong reflections can introduce significant errors in the localization process by creating deep fades and signal

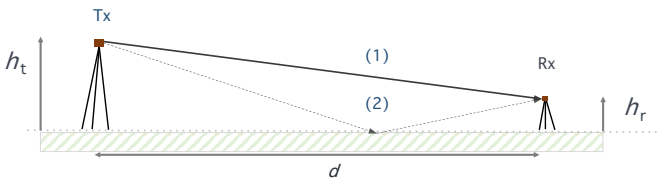

Fig. 1: The classical two-ray model showing (1) the direct line-of-sight (LoS) path, and (2) the ray reflected on the surface.

distortions that classical schemes do not address adequately. Understanding how these reflections influence the accuracy of WLS-based localization is crucial, especially in environments where such conditions are prevalent (e.g., water environments). This paper aims to fill this gap by analyzing the effects of the two-ray ground reflection model on localization accuracy, providing insights into the performance of WLS in the presence of strong reflected signals, and proposing potential strategies to mitigate these effects.

The remainder of this paper is structured as follows: Section II overviews the motivation and provides background on channel modeling and the WLS method. Section III describes the simulation setup, and Section IV discusses the results of our simulative assessment. Finally, Section V concludes the paper and outlines potential directions for future research.

II. Background & Motivation

Motivation: As the two-ray propagation model can reasonably well describe real-world RSS-based measurements in IoT settings dominated by surface reflections (e.g., in water environments [7], [8]), we will consider synthetic RSS data generated according to this model. Then, assuming a WLS regression method is applied to this RSS data to estimate the 2D position, we will consider a log-distance propagation model to fit the data. Note that this is a common way to apply WLS regression in practice (see, e.g., [5], [6]) as transforming the RSS-distance relationship into a log-linear form simplifies the estimation process. For completeness and considering the above observations, we will overview these concepts as a common introductory background in the following subsections.

A. The two-ray propagation model

We consider a point-to-point link of distance d with transmitter and receiver antennas positioned at the same height w.r.t. the ground surface, i.e., h=h_r=h_t as the scenario depicted in Fig. 1. This basic setup represents any anchor-target height-distance link configuration discussed in this paper. Assuming the two-ray model governs the underlying path loss behavior of these links, the signal strength at the receiver will result from the vectorial summation of two copies of the same transmitted signal that arrive at the receiver following two different paths: i) a direct line-of-sight (LoS) path between the transmitter and the receiver, and ii) an indirect path, reflected from the surface. The resulting self-interference pattern between these two signals will vary constructively or destructively, depending on the difference in their path lengths and the geometrical relationship to the antenna heights.

Formally, the two-ray propagation model in its simplified way [9] can be expressed in terms of the received power P_r as follows:

$$P_r = \frac{\lambda^2}{(4\pi d)^2}\left[2\sin\left(\frac{2\pi h_t\, h_r}{\lambda d}\right)\right]^2 P_t G_t G_r \tag{1}$$

where λ is the wavelength, P_t the transmitted power, and G_t and G_r the respective transmitter and receiver antenna gains.

B. The log-distance-model-based fitting

We consider a simple localization architecture in which a single target obtains the RSS data from different anchors and gets a distance estimate to each of them, assuming a log-distance path loss model [9]. This translates into a sequence of K consecutive RSS values collected by the target as in [5]. Each RSS value is denoted by $\{p_i\}$, where $i = 1, 2, \cdots N_{anch}$. Under this assumption, the distance estimates $\hat{d}_i$ and the measured RSS p_i are related by:

$$p_i = p_0 - 10n\log_{10}\hat{d}_i + \varepsilon_i \tag{2}$$

where p_0 is the power received at a reference distance and n is the path loss exponent. The term $\varepsilon_{i,k} \sim \mathcal{N}(0, \sigma^2)$ represents an additive noise component accounting for stochastic propagation effects such as shadowing or scattering. By neglecting this term, the estimated distance between the target and the i-th anchor can be directly derived by inverting (2), yielding:

$$\hat{d}_i \simeq 10^{\frac{\overline{p}_i - p_0}{10n}} \tag{3}$$

Upon estimating all distances, the target's 2D position can be determined using a multilateration-based algorithm.

C. Weighted least square (WLS) regression

The WLS [6] method extends the classical LS technique by incorporating weights that reflect the reliability of different measurements. These weights can account for various factors (e.g., environmental obstacles) by assigning higher weights to more reliable measurements and lower weights to less reliable ones, leading the WLS algorithm to generate more accurate estimates than methods that treat all measurements equally.

To illustrate this method, consider a subset of $N \subset N_{\text{anch}}$ with coordinates $\boldsymbol{a}_i$ and their corresponding estimated distances from the target denoted as $\hat{d}_i$. The WLS method involves solving a system of equations defined by the matrix $\boldsymbol{A}$ and the vector $\boldsymbol{b}$, as shown below:

$$\boldsymbol{A} = \begin{bmatrix} -2\boldsymbol{a}_1^T & 1 \\ -2\boldsymbol{a}_2^T & 1 \\ \vdots & \vdots \\ -2\boldsymbol{a}_N^T & 1 \end{bmatrix} \qquad \boldsymbol{b} = \begin{bmatrix} \hat{d}_1^2 - ||\boldsymbol{a}_1||^2 \\ \hat{d}_2^2 - ||\boldsymbol{a}_2||^2 \\ \vdots \\ \hat{d}_N^2 - ||\boldsymbol{a}_N||^2 \end{bmatrix} \tag{4}$$

Additionally, a diagonal weight matrix $\boldsymbol{W}$ is considered, with elements representing the inverse of the variance (σ^2)[1] of the squared estimated distances $\hat{d}_i^2$. This is defined by

$$\boldsymbol{W} = \text{diag}\left[\frac{1}{\sigma^2(\hat{d}_1^2)}, \frac{1}{\sigma^2(\hat{d}_2^2)}, \ldots, \frac{1}{\sigma^2(\hat{d}_N^2)}\right] \tag{5}$$

where $\sigma^2(\hat{d}_i^2)$ is computed as

$$\sigma^2(\hat{d}_i^2) = d_i^4 \exp\left(\frac{\sigma^2}{4.715n^2}\right)\left[\exp\left(\frac{\sigma^2}{4.715n^2}\right) - 1\right] \tag{6}$$

Finally, with all these parameters defined, the node's position can be estimated using the output of the WLS algorithm as:

$$\hat{\boldsymbol{\varrho}} = \left(\boldsymbol{A}^T\boldsymbol{W}\boldsymbol{A}\right)^{-1}\boldsymbol{A}^T\boldsymbol{W}\boldsymbol{b} \qquad \hat{\boldsymbol{t}} = [\hat{\varrho}_1, \hat{\varrho}_2]^T. \tag{7}$$

[1]Note that in this paper we are dealing with purely deterministic two-ray channel model, thus leaving all the related stochastic details for future work.

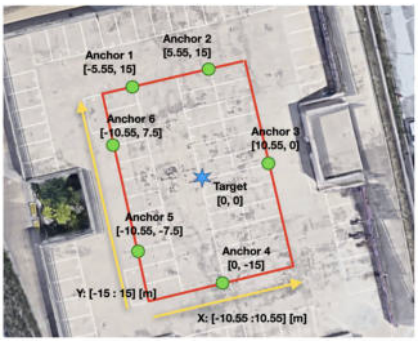

Fig. 2: Aerial view of "Scenario A" taken from [5] showing the target (blue star) and anchors (green dots) positions.

III. Simulation Setup

Data generation: The simulation dataset is generated synthetically assuming the two-ray model equation (1). This data simulates anchor-target distances according to the physical configuration presented in Fig. 2. In all cases, we consider a carrier frequency of 2.4 GHz, a localization area of 10.55×15 m2, with both anchors and target positioned coplanar in the vertical axis. The number of anchors is set to 6, positioned at the same 2D coordinates used in [5].

Data processing: The localization process comprises two parts. First, a fitting procedure is performed, in which we retrieve the data at selected distances and apply a linear regression to obtain the parameters p_0 and n for the log-distance model. Then, the position estimation procedure is applied, in which, assuming the log distance model, we estimate the target distance to each anchor from the RSS measurements and perform a WLS regression to obtain the target position.

IV. Simulation Results

We perform four experiments. Exp. 1 and Exp. 2 deal with localization errors versus distance for two distinguishing cases. The first assumes the baseline setup from Fig. 2 assessing the localization error across the area available. This experiment aims to show the case of "good" fitting since the estimated channel model is close to the original path loss data (see Fig.3). The second case is equivalent, yet it assumes a different antenna height. This case is referred to as "bad" fitting since the estimated channel model differs greatly from the nominal path loss (see Fig.4). Exp. 3 assesses both anchors and target antenna heights varying simultaneously, and Exp. 4 explores the impact of removing anchors that are retained "invalid".

A. Exp. 1: Localization errors vs. distance ("good" fitting)

We consider a height of 1.5m for the target and anchors, as in [5]. The log-distance parameters p_0 and n were obtained by applying linear regression to the synthetic two-ray RSS data over a set of given distances: $5, 10, 15, 20$ and 25 m, as illustrated in Fig. 3. For the synthetic data, we set -80 dBm as the minimum possible measured RSS value by each anchor.

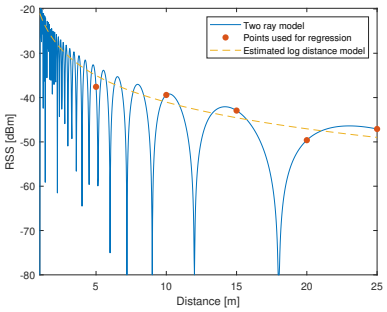

Fig. 3: Log-distance fitting for $h_{anchors} = h_{target} = 1.5[m]$.

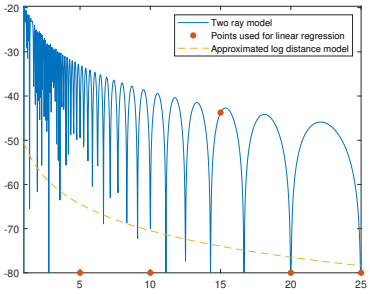

Fig. 4: Log-distance fitting for $h_{anchors} = h_{target} = 2.5[m]$.

We perform the localization for various target positions, ranging from -10.5 to 10.5 in the X-axis and from -15 to 15 in the Y-axis, separated by 0.5m for both axes, making 2623 simulations in total. The MSE of the localization for each simulation is displayed in Fig. 5a. The results show the error varies greatly for different target positions, for some areas being higher than the maximum possible distance between two points in the scenario $d_{max} \approx 36.68$m. To get some insight into the causes behind the error, we display the two-ray RSS measurements and the expected log-distance values for the corresponding anchor-target distance of each anchor at two given target positions. Fig. 6 shows these values for the target at $[0, 0]$, where the target is estimated to be at $[2.715, -1.773]$ with an MSE of 3.243, and Fig. 7 for the target at $[6, 2]$, where the target is estimated to be at $[699.3, 2388]$ with an MSE of 2484.

Fig. 7 shows that when the target is located at $[6, 2]$, some of the anchor measurements correspond to distances in which the two-ray self-interference is destructive, resulting in values that diverge greatly from the log-distance model used for localization. In contrast, when the target is located at $[0, 0]$ (Fig. 6), every anchor-target distance stays reasonably far from two-ray minima. While these simulations provide extreme errors caused by the two-ray model's deep fades, that would hardly be reached in an experimental setting. They illustrate how the algorithm may be heavily impacted when ground reflections are severe.

In order to mitigate the error values obtained in our previous

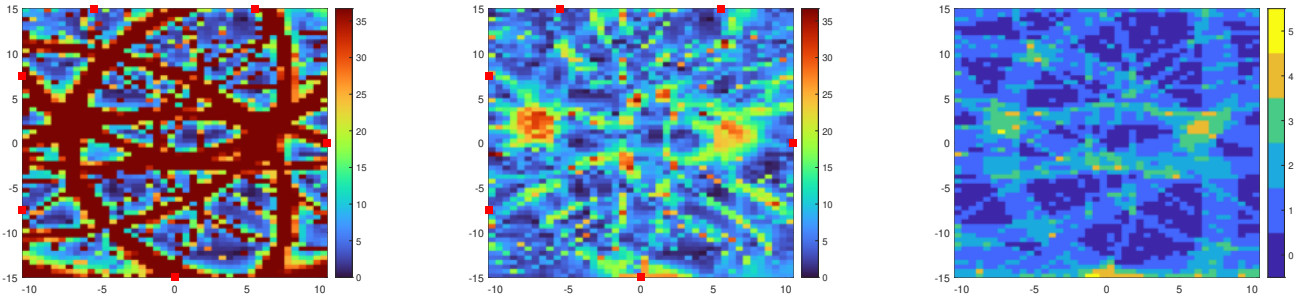

(a) MSE of the localization considering a minimum RSS of -80dBm for each anchor.

(b) MSE of the localization limiting the maximum distance to $36.68[m]$ for each anchor.

(c) Number of invalid anchors for each target position.

Fig. 5: Localization for different target positions, with $h_{anchors} = h_{target} = 1.5[m]$.

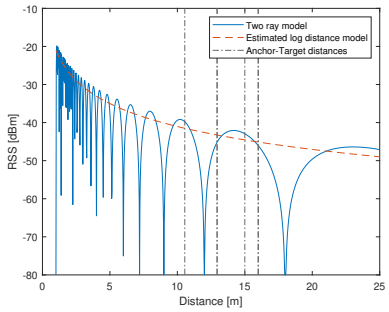

Fig. 6: Target-anchor distances for target at $[0, 0]$

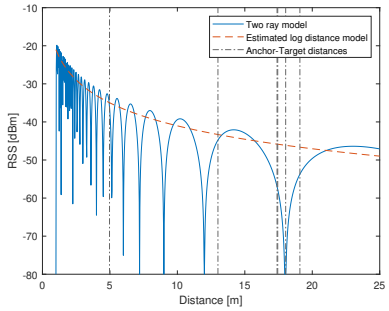

Fig. 7: Target-anchor distances for target at $[6, 2]$

simulations, we repeat the same experiment but taking into account the fact that the target is located inside the area delimited by the anchors. As the maximum distance between two points located within this rectangle is $d_{max} \approx 36.68$m, any target-anchor distance measurement superior to this value can be considered a product of ground reflection and will be set to d_{max}. Additionally, its corresponding anchor will be labeled as "invalid". In this case, for each target position, the localization MSE is displayed in Fig. 5b, and the amount of invalid anchors is displayed in Fig. 5c. As shown by Fig. 5b, the error is generally reduced when we limit the anchors' distance; however, it remains significant for an important part of the scenario. Fig. 5c graphically shows a strong correlation between the number of invalid anchors and the MSE.

B. Exp. 2: Localization errors vs. distance ("bad" fitting)

We now repeat the previous experiment, except changing the target and anchors antenna's height to 2.5m. The same set of distances is used to obtain the log distance model parameters. However, as shown by Fig. 4, most of the distances used for the linear regression correspond to points in which the self-interference is destructive, resulting in weak RSS measurements and poor fitting for the log distance model.

The localization MSE is displayed in Fig. 9, which shows good results near the center of the scenario and greater errors near the edges. However, as Fig. 10, which displays the estimated position for the target in every point of the simulated grid, shows, the algorithm localizes the target near the center no matter its real position, providing a poor localization performance.

These simulations illustrate that in addition to the impact of the ground reflections for the anchor measurements in the localization process, the fitting process may also be affected.

C. Exp. 3: Localization errors vs. antenna heigths

We place the target at position $[0, 0]$ and perform the localization procedure for various target and anchors' heights, ranging from 0.5 m to 4 m, separated by 0.1 m each, making a total of 1296 anchor-target height combinations. For each combination, we obtain a log-distance model using linear regression over a set of distances of $5, 10, 15, 20$, and 25 m, and we use the WLS algorithm to estimate the target position according to our log-distance model.

Similarly to Exp. 1, the localization was first performed using the raw distance estimate for each anchor (assuming -80 dBm as the minimum possible RSS measurement) as displayed in Fig. 8a, and then limiting the measured anchor target distance to $d_{max} \approx 36.68$m, as displayed in Fig. 8b. Fig. 8c shows the number of "invalid" anchors for each target-anchor height combination.

The results obtained in this experiment illustrate that for a given target position, the height of the antenna for the anchors and the target greatly affects the localization error

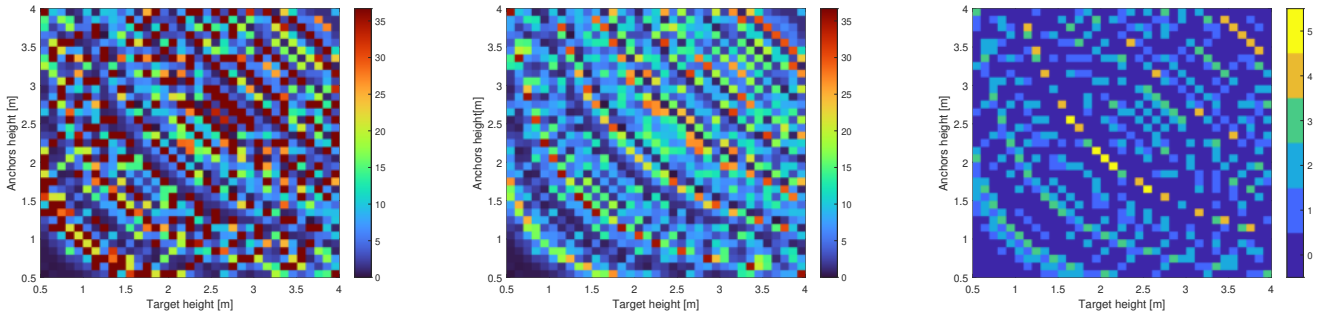

(a) MSE of the localization considering a minimum RSS of -80dBm for each anchor.

(b) MSE of the localization limiting the maximum distance to 36.68m for each anchor.

(c) Number of invalid anchors for each target position.

Fig. 8: Localization for different anchor and target heights, with target position at $[0, 0]$.

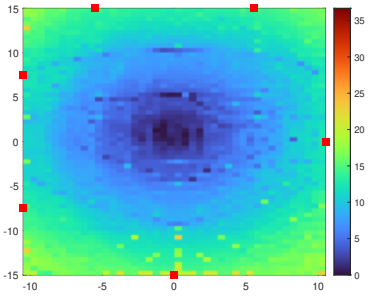

Fig. 9: Localization MSE for different target positions, with $h_{anchors} = h_{target} = 2.5[m]$.

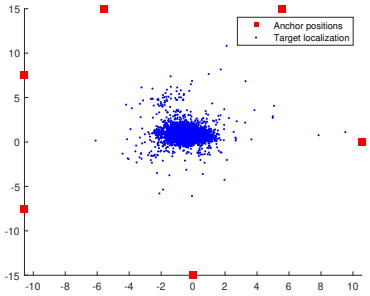

Fig. 10: Target localization results for different target positions, with $h_{anchors} = h_{target} = 2.5[m]$.

caused by ground reflections. This can be mitigated by limiting the maximum possible anchor-target distance, but even then, it remains highly significant for various cases. Additionally, we can observe a correlation between the number of invalid anchors and the MSE.

D. Exp. 4: Localization errors vs. # of valid anchors

Fig. 5 and Fig. 8 graphically show, for experiments 1 and 3, respectively, some correlation between the number of invalid anchors and the MSE of the target localization. This relationship is portrayed more explicitly in Fig. 11, which, considering the data of the simulations corresponding to experiment 3 with limited anchor distance (data from Fig. 8b), exhibits the MSE of the localization in relation to the number of invalid anchors. As the figure shows, the MSE generally rises when the number of invalid anchors is higher.

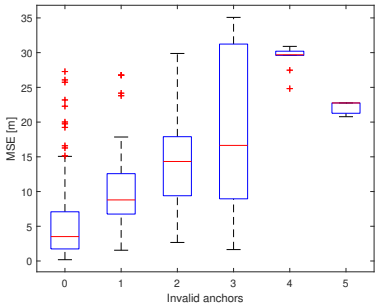

Fig. 11: MSE of the localization vs. number of invalid anchors.

As our simulations induce that the invalid anchors contribute to the localization error, we now repeat experiments 1 and 3, but only taking the valid anchors into account when the WLS algorithm is performed. It is worth noting that to be able to perform localization in a 2-D plane, we need at least three anchor measurements. Therefore, for these experiments, the configurations in which 4 or more anchors are deemed "invalid", will not be able to provide a localization result.

The localization errors vs. distance experiment, in which we simulate the localization under similar conditions to experiment 1, varying the target position throughout the scenario, is displayed in Fig. 12, while the localization errors vs. height experiment, in which we simulate the localization under similar conditions to experiment 3, positioning the target at $[0, 0]$ and varying the anchors and target antenna heights, is displayed in Fig. 13.

Figures 12 and 13 show that filtering the invalid anchors does in fact diminish the error of the estimation. However, it remains significant for select target positions or target-anchor height combinations. Additionally, there are 40 points in Fig. 12 and 18 points in Fig. 13, in which the amount of

valid anchors was not sufficient to perform the localization, therefore the amount of total anchors has to be taken into consideration for elimination based localization techniques.

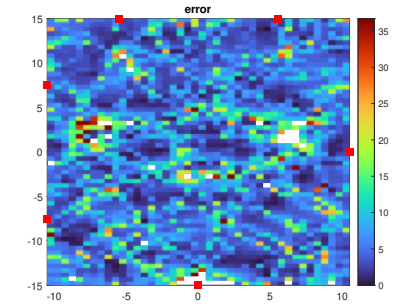

Fig. 12: MSE of the localization when filtering invalid anchors for different target positions and $h_{anchors} = h_{target} = 1.5[m]$.

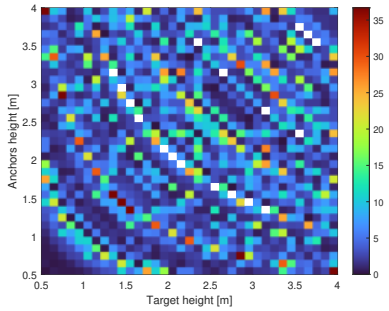

Fig. 13: MSE of the localization for different anchors and target heights at $[0, 0]$ when filtering the invalid anchors.

Finally, a summary of the simulation results is presented in Table I, which includes the average MSE for all target positions in the localization errors vs. distance experiment, and the average MSE for all height combinations in the localization error vs. height experiment. The average MSE was calculated for the three main modes of operation in these experiments: using the raw distance estimates, limiting the distance estimates to d_{max}, and eliminating the invalid anchors whose measurements exceed d_{max}. For the latter mode, cases where the number of valid anchors was insufficient for localization were ignored. As shown in the table, a pseudo-elimination of the invalid anchors can significantly improve target localization; however, the error due to two-ray ground reflections remains considerable overall.

TABLE I: Average MSE [dBm] for the localization error vs. distance and localization error vs. height experiments.

	Raw Distance	**Limited Distance**	**Filtered Anchors**
Error vs. Distance	253.55	9.0152	6.9701
Error vs. Height	151.96	8.3922	5.8957

V. Conclusions

This paper analyzed the impact of signal reflections on the accuracy of RSS-based localization for IoT devices using the WLS regression algorithm within a two-ray propagation model. Simulations with realistic WiFi/BLE settings revealed that localization accuracy is heavily influenced by deep fades from surface reflections, with errors depending on the geometry of the anchor-target positions. A simple pseudo-outlier elimination approach based on feasible localization distances was shown to significantly reduce these errors.

Future work will focus on leveraging the interaction between the propagation channel and RSSI-based localization to enhance WLS performance within an Integrated Sensing and Communication (ISAC) framework. Additionally, we aim to explore novel methods that utilize unique features of the two-ray channel, such as null spacing, to improve localization accuracy. These efforts target GPS-free localization in environments where GPS is unavailable due to environmental factors or jamming. Further research will also investigate the integration of reconfigurable intelligent surfaces (RIS) in two-ray channel scenarios, with a particular emphasis on applications like buoy and surface vehicle localization in overwater settings.

Acknowledgment

This work was supported by the FONDECYT Iniciación project No. 11241221 and the Competence Center START 4.0 under the Safepath project (CUP: J57H24000330004); also by the CISTER Research Unit (UIDP/ UIDB/04234/2020) through FCT/MCTES (Portuguese Foundation for Science and Technology) National Funds.

References

[1] Y. Li, Y. Zhuang, X. Hu, Z. Gao, J. Hu, L. Chen, Z. He, L. Pei, K. Chen, M. Wang *et al.*, "Toward location-enabled IoT (LE-IoT): IoT positioning techniques, error sources, and error mitigation," *IEEE Internet of Things Journal*, vol. 8, no. 6, pp. 4035–4062, 2020.

[2] P. S. Farahsari, A. Farahzadi, J. Rezazadeh, and A. Bagheri, "A survey on indoor positioning systems for IoT-based applications," *IEEE Internet of Things Journal*, vol. 9, no. 10, pp. 7680–7699, 2022.

[3] S. Sadowski and P. Spachos, "RSSI-based indoor localization with the Internet of things," *IEEE Access*, vol. 6, pp. 30 149–30 161, 2018.

[4] T. Janssen, R. Berkvens, and M. Weyn, "Benchmarking RSS-based localization algorithms with LoRaWAN," *Internet of Things*, vol. 11, p. 100235, 2020.

[5] G. Pettorru, V. Pilloni, and M. Martalò, "A hybrid WiFi/Bluetooth RSS dataset with application to multilateration-based localization," in *2023 IEEE International Mediterranean Conference on Communications and Networking (MeditCom)*. IEEE, 2023, pp. 293–298.

[6] B. Mukhopadhyay, S. Srirangarajan, and S. Kar, "RSS-based localization in the presence of malicious nodes in sensor networks," *IEEE Transactions on Instrumentation and Measurement*, vol. 70, pp. 1–16, 2021.

[7] M. G. Gaitán, P. M. Santos, L. R. Pinto, and L. Almeida, "Experimental evaluation of the two-ray model for near-shore WiFi-based network systems design," in *2020 IEEE 91st Vehicular Technology Conference (VTC2020-Spring)*. IEEE, 2020, pp. 1–3.

[8] M. G. Gaitán, P. M. d'Orey, J. Cecílio, M. Rodrigues, P. M. Santos, L. Pinto, A. Oliveira, A. Casimiro, and L. Almeida, "Modeling LoRa communications in estuaries for IoT environmental monitoring systems," *IEEE Sensors Journal*, vol. 22, no. 21, pp. 21 312–21 325, 2022.

[9] T. Rappaport, *Wireless Communications: Principles and Practice*, 2nd ed. USA: Prentice Hall PTR, 2001.